TU Delft

Delft University of Technology

Interleaved AC/DC Converter Operating with ZVS Sinusoidal Triangular-Current-Mode (S-TCM) for Reduced Voltage Harmonics Generation

Wu, Yang; Qin, Zian; Soeiro, Thiago Bastia; Bauer, Pavol

DOI
10.1109/ECCE53617.2023.10362205

Publication date
2023

Document Version
Final published version

Published in
2023 IEEE Energy Conversion Congress and Exposition, ECCE 2023

Citation (APA)
Wu, Y., Qin, Z., Soeiro, T. B., & Bauer, P. (2023). Interleaved AC/DC Converter Operating with ZVS Sinusoidal Triangular-Current-Mode (S-TCM) for Reduced Voltage Harmonics Generation. In *2023 IEEE Energy Conversion Congress and Exposition, ECCE 2023* (pp. 161-167). (2023 IEEE Energy Conversion Congress and Exposition, ECCE 2023). IEEE. https://doi.org/10.1109/ECCE53617.2023.10362205

Important note
To cite this publication, please use the final published version (if applicable).
Please check the document version above.

Copyright
Other than for strictly personal use, it is not permitted to download, forward or distribute the text or part of it, without the consent of the author(s) and/or copyright holder(s), unless the work is under an open content license such as Creative Commons.

Takedown policy
Please contact us and provide details if you believe this document breaches copyrights.
We will remove access to the work immediately and investigate your claim.

This work is downloaded from Delft University of Technology.
For technical reasons the number of authors shown on this cover page is limited to a maximum of 10.

Green Open Access added to TU Delft Institutional Repository

'You share, we take care!' - Taverne project

https://www.openaccess.nl/en/you-share-we-take-care

Otherwise as indicated in the copyright section: the publisher is the copyright holder of this work and the author uses the Dutch legislation to make this work public.

2023 IEEE Energy Conversion Congress and Exposition (ECCE) | 979-8-3503-1644-5/23/$31.00 ©2023 IEEE | DOI: 10.1109/ECCE53617.2023.10362205

Interleaved AC/DC Converter Operating with ZVS Sinusoidal Triangular-Current-Mode (S-TCM) for Reduced Voltage Harmonics Generation

Yang Wu[1], Zian Qin[1], Thiago Bastia Soeiro[2] and Pavol Bauer[1]
[1] DCE&S Group, Delft University of Technology, The Netherlands
[2] PE Group, University of Twente, The Netherlands
Email: Y.Wu-6@tudelft.nl; Z.Qin-2@tudelft.nl; t.batistasoeiro@utwente.nl; P.Bauer@tudelft.nl

***Abstract*—The sinusoidal Triangular-Current-Mode (S-TCM) method has been proposed in the AC/DC power-factor-correction (PFC) converter to achieve the zero-voltage-switching (ZVS) which can lead to both, high efficiency operation and a high power density design. Nevertheless, the necessary wide range variation of the sinusoidal switching frequency profile imposed by the S-TCM results in a larger generated voltage harmonic peak due to the overlapping between different order carrier-frequency harmonics. In this work, the S-TCM is used in the interleaved 2-level converter to minimize the undesirable effects of such overlapped voltage harmonics while maintaining ZVS via S-TCM. Meanwhile, the necessity of coupled inductors (CIs) in the interleaved topology is avoided by implementing the S-TCM. Both simulation and experimental tests conducted in a 3.3 kW interleaved 2-level converter system are used to verify the study.**

***Index Terms*—Sinusoidal Triangular-Current-Mode (S-TCM), Zero-voltage-switching (ZVS), Interleaved AC/DC converter, harmonic spectrum.**

I. Introduction

Due to the rapid development of the renewable energy integration and E-mobility, Pulse Width Modulation (PWM)-based Voltage Source Converters (VSCs) play a critical role in the associated grid-connection applications because of their robustness and simplicity. In recent years, there are more and more research efforts put in various modulation techniques to improve the converter efficiency or to reduce the magnetic part, for a more compact and efficient AC/DC power-factor-correction (PFC) converter system.

Typically the frequency modulation methods adopted in the literatures, for instance the TCM and S-TCM methods [1]–[8] for the zero-voltage switching (ZVS) operation in AC/DC converter, exhibit a periodicity and variation in the switching frequency. The wide range of switching frequency results in the overlapping between the different order carrier-frequency harmonics generated by the VSC and the consequently increased harmonic peak generated might violate the related supra-harmonics standards [9], [10], as depicted in Fig. 1. By increasing the VSC input-to-output voltage conversion ratio, namely the modulation index, for example by means of third-harmonics injection, the overlap between the spectra can be minimized to some extend because of the reduced frequency variation range. However, this complicates the design of the power conversion placed after the VSC stage.

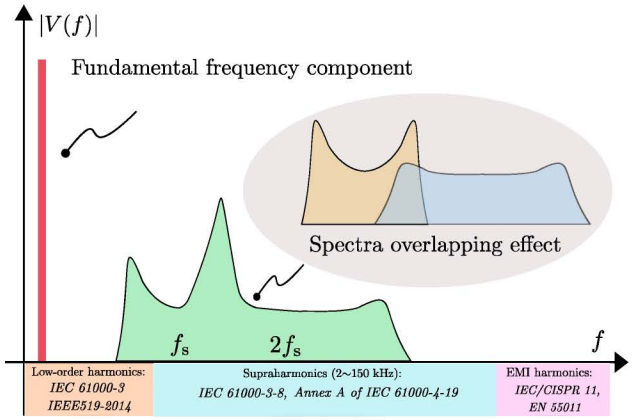

Fig. 1. Overlapping between harmonics under S-TCM.

Besides, the wide range of switching frequency can also cause the considerable harmonics clustered in the Electromagnetic-interference (EMI) range. The 2-Interleaved topology cancels the odd order carrier-frequency harmonics as shown in Fig. 2, and hence can be implemented with TCM/S-TCM to avoid the harmonics overlapping and reduce the high frequency current harmonics while achieving the desired ZVS operation. In contrast to the conventional 2-interleaved converter, the coupled inductors (CIs) used to suppress the circulating current are not required by the TCM/S-TCM methods since the two interleaved currents in one phase will not be deviated by the circulating current. Compared to the TCM method, S-TCM uses a simpler switching frequency profile with much less frequency variation range (sinusoidal), which results in a better harmonics spectra and it is more easily to be digitally implemented. Therefore, the interleaved S-TCM is used to reduce

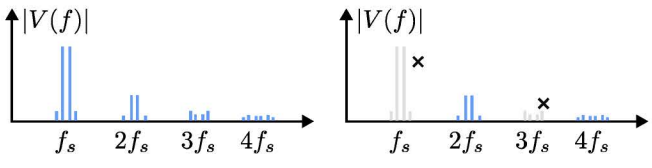

(a) Non-interleaving. (b) 2-interleaving.

Fig. 2. Output voltage harmonics of PWM converter.

Authorized licensed use limited to: TU Delft Library. Downloaded on April 03,2024 at 06:42:32 UTC from IEEE Xplore. Restrictions apply.

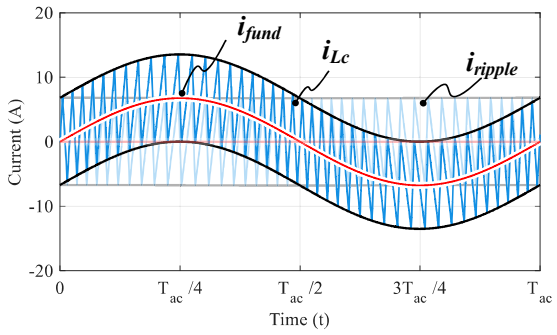

(a) Inductor current generated by S-TCM.

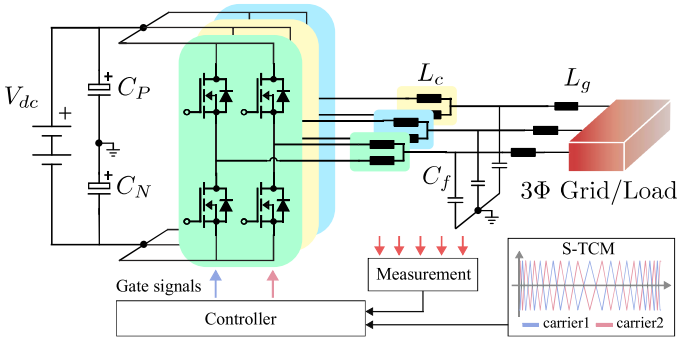

(b) Three-phase 2-interleaved PWM converter with S-TCM.

Fig. 3. S-TCM method and the implemented topology.

TABLE I
SYSTEM PARAMETERS FOR SIMULATION AND EXPERIMENT

PARAMETER	VALUE
Grid interface	
Voltage $V_{\rm ac}$ (rms)	230 V
Fundamental frequency f_o	50 Hz
Converter-side inductance $L_{\rm c}$	360 μH
Grid-side inductance $L_{\rm g}$	720 μH
$C_{\rm f}$	5 μF
Converter	
Semiconductor	IKW15N120BH6
Blocking voltage $V_{\rm B}$	1200 V
Collector current $I_{\rm C}$	15 A ($T_{\rm c}=100°$)
Operating power	3.3 kW
$V_{\rm dc}$	700 V
$C_{\rm dc}$	365 μF
$f_{\rm c0}$	40.85 kHz
$f_{\rm swb}$	31.05 kHz
Modulation	
PWM	SPWM
Frequency profile	Sinusoidal (S-TCM)

the output switching harmonics. The analytical model of the harmonic spectra due to the sinusoidal switching frequency is derived for the filter design. Simulations and preliminary experiment are conducted in a 3.3 kW system for verification.

II. S-TCM IN 2-INTERLEAVED CONVERTER

A. S-TCM for ZVS Operation

The implementation of S-TCM in a half-bridge converter is shown in Fig. 3. The current flowing through $L_{\rm c}$ is a sinusoidal current $i_{\rm ac}$ (or $i_{\rm g}$ neglect capacitor influence) superposed with a constant ripple band $i_{\rm band}=2\hat{I_{\rm ac}}$. Generally, the switch-on and switch-off time during one switching cycle can be expressed by:

$$\begin{aligned} T_{\rm on}(t) &= \frac{2L_{\rm c}i_{\rm band}}{V_{\rm dc}(1-M\cos(\omega_{\rm o}t))} \\ T_{\rm off}(t) &= \frac{2L_{\rm c}i_{\rm band}}{V_{\rm dc}(1+M\cos(\omega_{\rm o}t))} \end{aligned} \tag{1}$$

The switching frequency hence can be derived as:

$$\begin{aligned} f_{\rm sw}(t) &= \frac{V_{\rm dc}}{4L_{\rm c}i_{\rm band}}\cdot\left[1-M^2\cos^2(\omega_{\rm o}t)\right] \\ &= f_{\rm sw0}-f_{\rm swb}\cdot\cos(2\omega_{\rm o}t) \\ &= f_{\rm sw0}+f_{\rm swb}\cdot\sin(2\omega_{\rm o}t+3\pi/2) \end{aligned} \tag{2}$$

where $\omega_{\rm o=2\pi\cdot 50}$ is the angular frequency of the grid and M is the modulation index expressed as: $M=2V_{\rm dc}/\hat{v}_{\rm g}$. The switching frequency varies with twice the fundamental frequency. The centered frequency $f_{\rm sw0}$ is inversely proportional to M^2 while the frequency variation band $f_{\rm swb}$ is opposite. For the two interleaved bridges, the output currents in the two bridges i_1 (and i_2) are superposed of a fundamental frequency component and the high-frequency triangle ripple with the constant band $i_{\rm band}$ as depicted in Fig. 3(a):

$$i_1=i_{\rm fund}+i_{\rm ripple}=\hat{I_{\rm ac}}\cdot(\cos(\omega_{\rm o}t)+i^*_{\rm ripple}) \tag{3}$$

where $i^*_{\rm ripple}$ is the unit ripple function determined by the switching frequency generated by S-TCM as expressed in (2). In each switching cycle, the upper bound of i_1 is larger than 0 and the lower bound is vice versa. Hence, the zero-crossing of the current forces the body diode of the switch take over the output current before the switch conducts. Therefore the zero-voltage-switching (ZVS) turn on is realized with S-TCM method.

It is noteworthy that the mid-point of the three phase capacitors is connected to the mid-point of the DC bus, which implies that the three phases can operated independently under S-TCM. Therefore, the three phases are fully decoupled from each other with S-TCM operation and the aforementioned analysis and switching profile can be directly applied to the three phases. However, it is worthy to mention that the switching frequency for the three phases should incorporate the difference of the phase angles between three phases.

Authorized licensed use limited to: TU Delft Library. Downloaded on April 03,2024 at 06:42:32 UTC from IEEE Xplore. Restrictions apply.

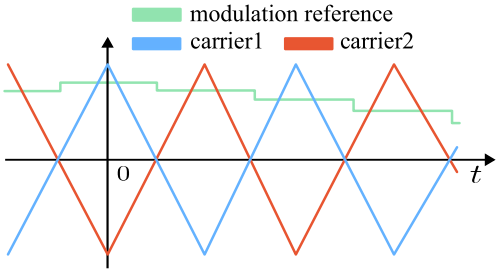

Fig. 4. Carrier-based PWM for interleaved 2-level PWM converter.

B. Circuitry Modeling of 2-Interleaved Converter

In the three-phase 2-interleaved converter depicted in Fig. 3(b), each phase requires two inductors L_c for the two interleaved switching bridges. For the carrier-based PWM implementation, the carrier signals for the two interleaved bridges are 180° phase-shifted while sharing the same modulation reference signal as shown in Fig. 4. For the power operation, the load (grid) power and current are shared equally between the interleaved bridges, hence for nominal power operation i_{band} is set to be the peak AC current ($i_{\text{band}} = \hat{I_{\text{ac}}}$). Generally i_{band} can be kept constant for different operating power levels. Alternatively, the current band can also follow a certain profile to optimize the conduction losses of the power semiconductor [1].

Since three phases are decoupled under S-TCM, the single-phase representation circuit is simplified as shown in Fig. 5(a) from the three-phase 2-interleaved power electronic circuit for simplicity of analysis. By applying Kirchhoff's voltage and current law (KVL and KCL) to this circuit, the following relation can be obtained:

$$\frac{v_{c1}+v_{c2}}{2} - v_C = \frac{L_c}{2}\cdot\frac{\mathrm{d}i_c}{\mathrm{d}t} \tag{4}$$

From the perspective of harmonics flowing into the grid, the circuit can be further transformed into Fig. 5(b) based on (3). The inductance contributing to the converter-side current i_c hence is halved to $L_c/2$ and v_{eq} is equal to $(v_{c1}+v_{c2})/2$. This implies that the source of the current switching harmonics is the average of the output voltage of the interleaved bridges.

It should be mentioned that the three-phase grid (load) has a 3-wire connection configuration. Therefore only the differential-mode (DM) current components can flow into the three-phase grid or load because of the inherently infinite impedance for the common-mode (CM) current components. From the perspective of harmonics emission and its associated filter design, only the DM harmonic components are concerned with the grid-side currents. Theoretically, the DM and CM components have the followings relations:

$$\begin{cases} x_a + x_b + x_c = 0 & \text{Differential-mode} \\ x_a = x_b = x_c & \text{Common-mode} \end{cases} \tag{5}$$

where x represents the three-phase voltages and currents in this circuit. Besides, the DM harmonic components of the converter output voltage can be expressed as:

$$v_{x,dm} = v_x - \frac{v_a+v_b+v_c}{3} \tag{6}$$

III. Harmonic Spectra Model under Interleaved S-TCM

The voltage harmonic spectra under any arbitrary periodic variable switching frequency profile as expressed by (7) has been derived for convention 2-level PWM converter by [11].

$$f_c(t) = f_{c0} + \sum_{k=1}^{\infty} C_k \sin(2\pi k f_m t + \theta_k) \tag{7}$$

In this work, the S-TCM has a sinusoidal frequency profile with a periodicity frequency $f_m = 2f_o$ and $\theta_k = 3\pi/2$ (k=1). By substitution, the voltage spectra generated by S-TCM in the 2-interleaved VSC is derived in (8).

$$v_{eq}(t) = \Re\Big(\sum_{m=0}^{\infty}\sum_{n=-\infty}^{\infty}\sum_{l=-\infty}^{\infty}\underbrace{\{C_{mnl}\cdot e^{j2\pi(mf_{c0}t+nf_ot+lf_mt)}\}}_{\text{m= 0, 2, 4, 6, 8}\cdots}\Big) \tag{8}$$

$$\begin{aligned} C_{mnl} &= C_{mn}J_l\Big(\frac{mC_1}{f_m}\Big)\cdot e^{j(\theta_{mn}+\varphi_m+l(\theta_1-\pi/2))} \\ &= C_{mn}J_l\Big(\frac{mf_{swb}}{2f_o}\Big)\cdot e^{j(\theta_{mn}+\varphi_m+l\pi)} \end{aligned} \tag{9}$$

where $J_n(x)$ is the Bessel function of the first kind and C_{mn} is the coefficient of the harmonics generated by the constant switching frequency under SPWM with the symmetrical sampling:

$$C_{mn} = \frac{2V_{dc}J_n[(m+n\frac{\omega_o}{\omega_{c0}})\frac{\pi M}{2}]}{\pi(m+n\frac{\omega_o}{\omega_{c0}})}\sin[(m+n\frac{\omega_o}{\omega_{c0}}+n)\frac{\pi}{2}] \tag{10}$$

and θ_{mn} and φ_m are expressed as:

$$\begin{aligned} \theta_{mn} &= m\theta_c + n\theta_o \\ \varphi_m &= \sum_{k=1}^{\infty}\frac{mC_k\cos(\theta_k)}{kf_m} \end{aligned} \tag{11}$$

With (8)–(11), the voltage harmonics spectra of the three-phase 2-interleaved PWM converter can be calculated and obtained under the S-TCM method. Once the filter parameters are known, the harmonics flowing to the grid side current i_g can be obtained through the following equations:

$$\begin{aligned} i_g(s) &= \frac{2v_{eq}(s)}{L_cL_gC_fs(s^2+\omega_{res}^2)} \\ \omega_{res} &= \sqrt{\frac{L_c+2L_g}{L_cL_gC_f}} \end{aligned} \tag{12}$$

It is noteworthy that v_{eq} contains both common-mode (CM) and differential-mode (DM) harmonics components. Since only DM current harmonics flow into the grid, the CM components must be removed from v_{eq} before applying (12), the use of which has been elaborated in [11] in details. The total inductance namely $L_c/2 + L_g$ hence can be selected to meet the current harmonic emission limit set by different

Authorized licensed use limited to: TU Delft Library. Downloaded on April 03,2024 at 06:42:32 UTC from IEEE Xplore. Restrictions apply.

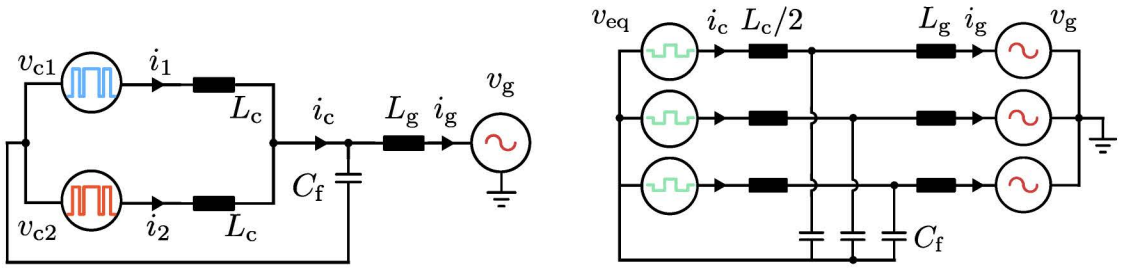

(a) Single-phase representation.

(b) Equivalent circuit seen by the load/grid.

Fig. 5. Circuit simplification of interleaved converter

standards such as IEEE-519 and IEC-61000-3. This can be done by limiting the magnitude of the critical current harmonic (most highest harmonic) to be the emission limit value and the inductance can be subsequently derived.

IV. Simulation and Experimental Verification

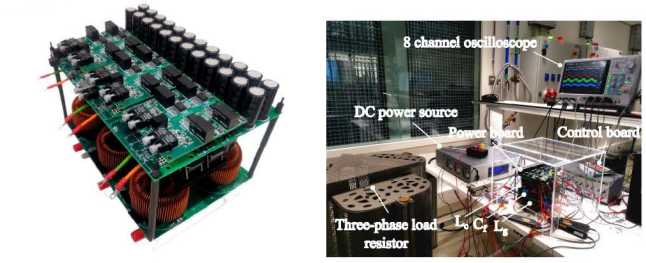

(a) Experiment prototype.

(b) Test-bench.

Fig. 6. Experimental set-up and test-bench.

In order to verify the S-TCM in the 2-interleaved PWM converter, both simulation and experimental tests are conducted in a 3.3 kW system with the operating parameters listed in Table I. Specifically, the simulation verification is done in PLECS while the experiment has been conducted in the three-phase 2-interleaved PWM converter with its test-bench shown in Fig. 7. Besides, the harmonic spectra of both simulation and experimental results are analyzed and compared in order to verify the correctness of the harmonic spectra model.

A. S-TCM for ZVS Operation

Based on the parameters listed in Table I, the S-TCM has the following switching frequency profile: $f_{sw0} = 40.85$ kHz and $f_{swb} = 31.05$ kHz. It should be noted that both f_{sw0} and f_{swb} in fact are not exactly multiples of f_o after calculated by (2). Hence they are selected to be their nearest multiples of f_o in order to avoid the inter-harmonics and non-multiple harmonics [10]. Fig. 8 shows the simulated waveforms generated by the interleaved and non-interleaved (hard-paralleling) S-TCM operations. In both cases, i_1 and i_2 have the same magnitude of ripple. However, they overlap in the non-interleaving case and oppose each other in the interleaved case, as it can be seen in Fig. 8. Because of the cancellation of the interleaved current ripples, the current i_c has a reduced current in interleaved operation compared to hard-paralleling case. It can be noted from Fig.7 that the current crosses zero in every switching cycle and hence ZVS is realized.

In experiment, only the voltage and current waveforms from Phase A are recorded due to limitation of oscilloscope channels. The experimental waveforms are presented in Fig. 9 for both hard Fig. 9 presents the recorded experimental

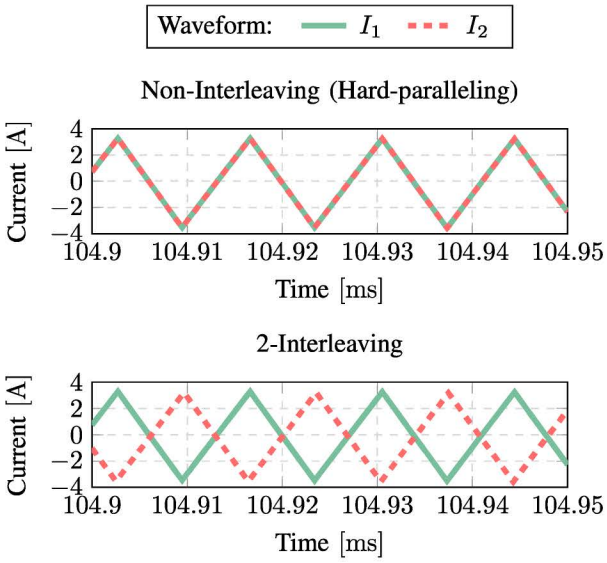

Fig. 7. Zoom-in waveforms.

waveforms under S-TCM for both 2-interleaving and non-interleaving operations. The zoomed-in waveforms also show the overlapped ripple under non-interleaving (hard-paralleling) case and the interleaved current ripples under 2-interleaving case. Specifically, the i_{band} waveform in both test cases is equal to I_{ac} (6.7 A). Besides, the current ripples of both i_{a1} and i_{a2} cross the zero point in each switching cycle, indicating the successful realization of ZVS operation.

B. Harmonic Spectra Verification

Based on the recorded converter output waveforms v_{ca1} and v_{ca2} under both 2-interleaving and non-interleaving operations, the harmonic spectra of the converter output voltages can be extracted through FFT analysis. Therefore, the converter output voltage harmonic spectra constructed by the analytical

Authorized licensed use limited to: TU Delft Library. Downloaded on April 03,2024 at 06:42:32 UTC from IEEE Xplore. Restrictions apply.

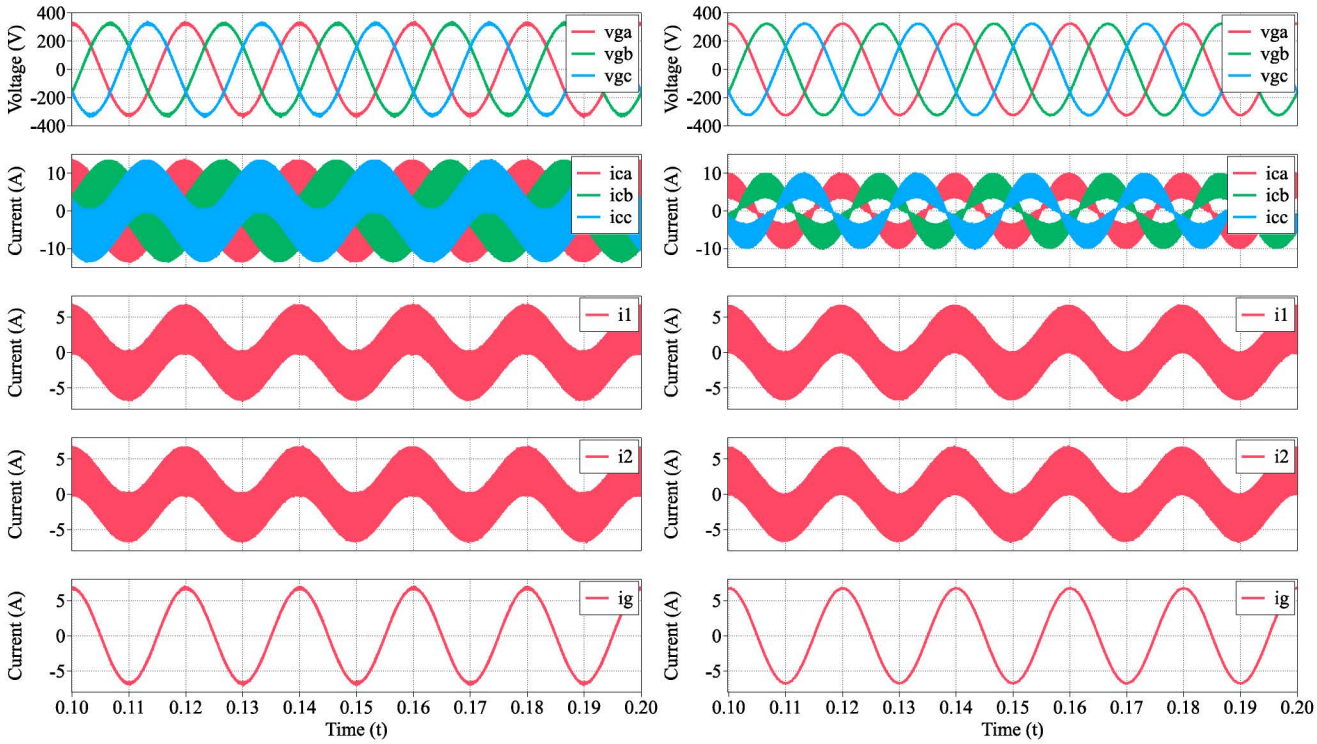

(a) Non-Interleaving (Hard-paralleling). (b) 2-Interleaving.

Fig. 8. Simulation waveforms.

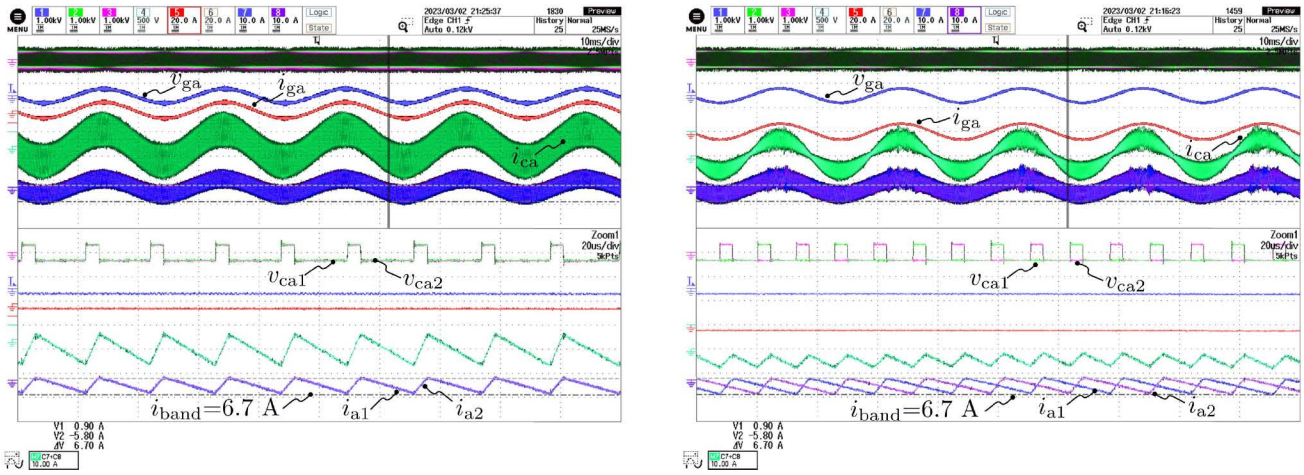

(a) Non-Interleaving (Hard-paralleling). (b) 2-Interleaving.

Fig. 9. Experimental waveforms.

models based on (8)–(11) is compared with both simulation and experimental results. It can be noted from Fig. 10 that the analytical voltage harmonic spectra matches the simulated one with a quite high accuracy for both interleaved and non-interleaved operations. The analytical result has some negligible difference from the experimental one but is also close to it. Therefore, the correctness of the harmonic spectra model is verified by both simulation and experimental results. The model hence is reliable to be used for the follow-up filter design to meet the harmonic emission standards.

C. Harmonic Emission Level

Fig. 11 presents the simulated three-phase grid currents and their harmonic spectra. It can be noted that the both the TDD (total-demand-distortion) and the peak switching harmonic of the grid current under 2-interleaving are significantly reduced

Authorized licensed use limited to: TU Delft Library. Downloaded on April 03,2024 at 06:42:32 UTC from IEEE Xplore. Restrictions apply.

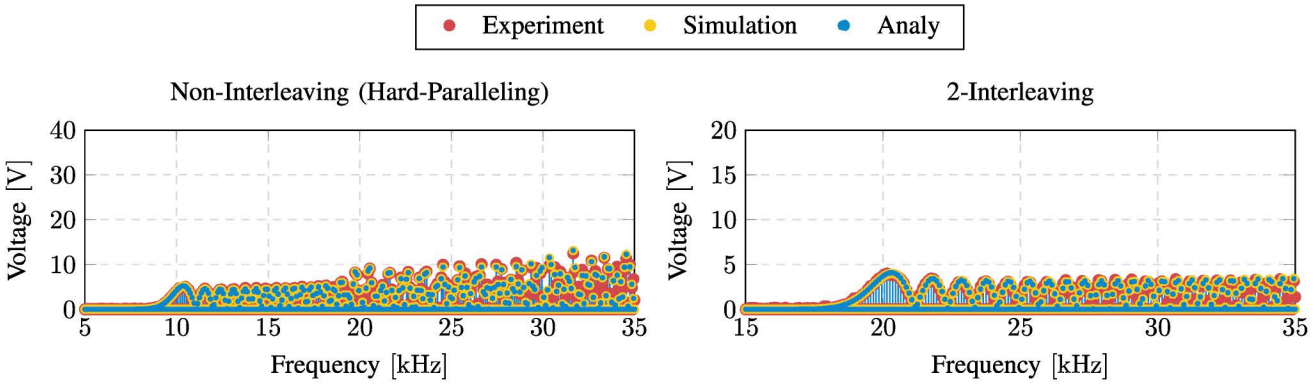

Fig. 10. Spectra comparison between analytical, simulation and experimental results: The voltage harmonic spectra (Phase A) under S-TCM for both interleaved and non-interleaved operations.

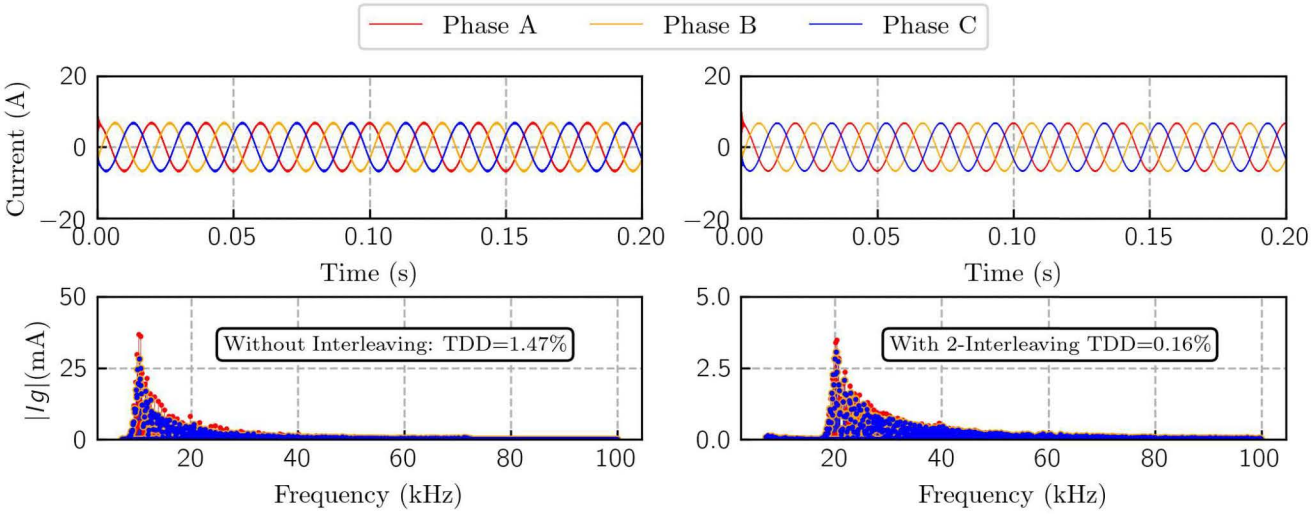

Fig. 11. Harmonic spectra of the three-phase grid currents.

compared to non-interleaving (9 times smaller). In other words, a much smaller required grid-side inductance L_g can be chosen for the interleaved operation to meet the current harmonic emission limits for the individual harmonics set by the standards.

V. Conclusion and Future Work

This work proposed the S-TCM ZVS operation in the interleaved converter to reduce the harmonic generation while maintaining the ZVS operation. Besides, the analytical harmonic spectra model is proposed for a follow-up design and study of the filter to meet the emerging supra-harmonics standards. Both simulation and experimental results verify that the ZVS is guaranteed under interleaved operation. Furthermore, the simulation results show that the peak harmonic of the output current is reduced by 9 times in interleaved operation compared to non-interleaved case. This implies the grid-side inductor in interleaved operation can be significantly reduced compared to non-interleaved case to meet the same current harmonic emission standard.

References

[1] M. Haider, J. A. Anderson, S. Mirić, N. Nain, G. Zulauf, J. W. Kolar, D. Xu, and G. Deboy, "Novel zvs s-tcm modulation of three-phase ac/dc converters," *IEEE Open J. of Power Electr.*, vol. 1, 2020.

[2] D. Rothmund, T. Guillod, D. Bortis, and J. W. Kolar, "99.1sic-based medium-voltage zvs bidirectional single-phase pfc ac/dc stage," *IEEE J. of Em. and Selec. Topics in Power Electr.*, vol. 7, no. 2, 2019.

[3] J. Chen, D. Sha, J. Zhang, and X. Liao, "A variable switching frequency space vector modulation technique for zero-voltage switching in two parallel interleaved three-phase inverters," *IEEE Transactions on Power Electronics*, vol. 34, no. 7, pp. 6388–6398, 2019.

[4] Z. Huang, Z. Liu, F. C. Lee, and Q. Li, "Critical-mode-based soft-switching modulation for high-frequency three-phase bidirectional ac–dc converters," *IEEE Transactions on Power Electronics*, vol. 34, no. 4, pp. 3888–3898, 2019.

[5] M. Haider, J. A. Anderson, N. Nain, G. Zulauf, J. W. Kolar, D. Xu, and G. Deboy, "Analytical calculation of the residual zvs losses of tcm-operated single-phase pfc rectifiers," *IEEE Open Journal of Power Electronics*, vol. 2, pp. 250–264, 2021.

Authorized licensed use limited to: TU Delft Library. Downloaded on April 03,2024 at 06:42:32 UTC from IEEE Xplore. Restrictions apply.

[6] J. Xu, T. B. Soeiro, Y. Wang, F. Gao, H. Tang, and P. Bauer, "A hybrid modulation featuring two-phase clamped discontinuous pwm and zero voltage switching for 99% efficient dc-type ev charger," *IEEE Transactions on Vehicular Technology*, vol. 71, no. 2, pp. 1454–1465, 2022.
[7] Q. Zhang, H. Hu, D. Zhang, X. Fang, Z. J. Shen, and I. Bartarseh, "A controlled-type zvs technique without auxiliary components for the low power dc/ac inverter," *IEEE Transactions on Power Electronics*, vol. 28, no. 7, pp. 3287–3296, 2013.
[8] C. Marxgut, F. Krismer, D. Bortis, and J. W. Kolar, "Ultraflat interleaved triangular current mode (tcm) single-phase pfc rectifier," *IEEE Transactions on Power Electronics*, vol. 29, no. 2, pp. 873–882, 2014.
[9] M. Bollen, M. Olofsson, A. Larsson, S. Rönnberg, and M. Lundmark, "Standards for supraharmonics (2 to 150 khz)," *IEEE Electromagnetic Compatibility Magazine*, vol. 3, no. 1, pp. 114–119, 2014.
[10] L. Wang, Z. Qin, T. Slangen, P. Bauer, and T. van Wijk, "Grid impact of electric vehicle fast charging stations: Trends, standards, issues and mitigation measures - an overview," *IEEE Open Journal of Power Electronics*, vol. 2, pp. 56–74, 2021.
[11] Y. Wu, J. Xu, T. B. Soeiro, M. Stecca, and P. Bauer, "Optimal periodic variable switching pwm for harmonic performance enhancement in grid-connected voltage source converters," *IEEE Transactions on Power Electronics*, vol. 37, no. 6, 2022.

Authorized licensed use limited to: TU Delft Library. Downloaded on April 03,2024 at 06:42:32 UTC from IEEE Xplore. Restrictions apply.